*geologica*acta

Chromite and platinum group elements mineralization in the Santa Elena Ultramafic Nappe (Costa Rica): geodynamic implications

F. ZACCARINI [1] **G. GARUTI** [1] **J.A. PROENZA** [2] **L. CAMPOS** [3] **O.A.R. THALHAMMER** [1] **T. AIGLSPERGER** [2] **J.F. LEWIS** [4]

[1] **Department of Applied Geosciences and Geophysics, University of Leoben**
Peter Tunner Str. 5, 8700 Leoben, Austria.   E-Mail: Federica.Zaccarini@unileoben.ac.at

[2] **Departament de Cristal·lografia, Mineralogia i Dipòsits Minerals, Facultat de Geologia, Universitat de Barcelona (UB)**
C/ Martí i Franquès s/n, E–08028 Barcelona, Spain

[3] **Escuela Centroamericana de Geología, University of Costa Rica**
San Pedro de Montes de Oca, 240-2060 UCR, San José, Costa Rica

[4] **Department of Earth and Environmental Sciences, The George Washington University**
2029 G St. NW, Washington, D.C. 20052, U.S.A.

─┤ **A B S T R A C T** ├─

Chromitites associated with strongly altered peridotite from six distinct localities in the Santa Elena ultramafic nappe (Costa Rica) have been investigated for the first time. Santa Elena chromitites commonly display a compositional variation from extremely chromiferous (Cr/(Cr+Al)=0.81) to intermediate and aluminous (Cr/(Cr+Al)=0.54). This composition varies along a continuous trend, corresponding to calculated parental liquids which may have been derived from the differentiation of a single batch of boninitic magma with Cr-rich and (Al, Ti)-poor initial composition. Fractional precipitation of chromite probably occurred during differentiation of the boninitic melt and progressive metasomatic reaction with mantle peridotite. The distribution of platinum group elements (PGE) displays the high (Os+Ir+Ru)/(Rh+Pt+Pd) ratio typical of ophiolitic chromitites and, consistently, the platinum group minerals (PGM) encountered are mainly Ru-Os-Ir sulfides and arsenides. Textural relations of most of the platinum group elements suggest crystallization at magmatic temperatures, possibly under relatively high sulfur fugacity as indicated by the apparent lack of primary Os-Ir-Ru alloys.

The chemical and mineralogical characteristics of chromitites from the Santa Elena ultramafic nappe have a strong affinity to podiform chromitites in the mantle section of supra-subduction-zone ophiolites. Calculated parental melts of the chromitites are consistent with the differentiation of arc-related magmas, and do not support the oceanic spreading center geodynamic setting previously proposed by some authors.

KEYWORDS | **Chromitite. Santa Elena Ultramafic Nappe. Costa Rica. Chromite composition. PGE-PGM. Geodynamic setting.**

INTRODUCTION

Recognition of the original geological setting of oceanic igneous complexes located along the Pacific coast of Costa Rica is at the focus of the geodynamic evolution of Central America (Fig. 1A). The northernmost of these complexes, located in Santa Elena Peninsula, has recently received contrasting interpretations, and the nature of its oceanic evolution has been a matter of debate. The Santa Elena complex may have been generated at an oceanic spreading center in a mantle plume region, analogous with the present Galapagos ridge/hot spot system (Beccaluva et al., 1999), or may represent the remnants of an inter-American proto-Caribbean ocean (Giunta et al., 2006). In contrast with these models, it has been proposed that the Santa Elena ophiolite complex was originally emplaced in a supra subduction zone, more precisely in an island arc setting (Hauff et al., 2000; Denyer et al., 2006; Gazel et al., 2006; Denyer and Gazel, 2009). Petrogenetic conditions of the ultramafic rocks of Santa Elena are difficult to determine due to the high degree of hydrothermal alteration and lateritic weathering. These processes have almost totally transformed the primary magmatic silicates into a secondary assemblage, mainly composed of serpentine, talc and chlorite, which hinder the identification of the original mantle lithology. In spite of such a deep mineralogical modification, the ultramafic block of Santa Elena contains small chromitite bodies which have visibly preserved a large part of their original magmatic character. This is due to the fact that chromian spinel is generally more resistant to alteration than mafic silicates. Although it may be transformed into secondary ferrian-chromite (Beeson and Jackson, 1969), its primary magmatic composition is usually preserved at the core of partially altered grains.

The potential of chromite (a chromian spinel with $Cr_2O_3 > \sim 40wt\%$) as a petrogenetic indicator has been recognized for more than 40 years. Chromite composition helps to distinguish podiform chromitite associated with residual mantle in ophiolite belts (ophiolitic chromitites) from stratiform chromitite in continental layered intrusions and from chromitite segregations in Ural-Alaskan type complexes (Irvine, 1965, 1967; Thayer, 1970). In particular, the composition of chromite from podiform chromitites depends on the type of parental magma (e.g.: MORB, OIB, boninite) and the degree of depletion of its mantle source. Chromitite has become a reliable indicator of the geodynamic setting in which the minerals and their host rock have formed (Dick and Bullen, 1984; Roeder, 1994; Stowe, 1994; Zhou and Robinson, 1997; Barnes and Roeder, 2001; Kamenetsky et al., 2001; Rollinson, 2008).

Ophiolitic chromitites are carriers of PGE, although at a sub-economic level (Garuti, 2004). They are especially enriched in Os, Ir, and Ru, when compared to their country rocks, but may display different PGE compositions depending on the nature of the parent melt and the geodynamic setting of the host mantle peridotite (Zhou et al., 1998, and references therein). The mineralogical expression of the PGE content are, the PGM, occurring as micrometric minerals unevenly disseminated in the chromitite. Primary PGM representing pristine magmatic phases, trapped into crystallizing chromite at high temperatures, can be used to evaluate specific thermodynamic conditions, such as sulfur fugacity and temperature prevailing in the magmatic system during the precipitation of chromite (Augé and Johan, 1988; Garuti et al., 1999b; Brenan and Andrews, 2001).

The chromitites of Santa Elena were initially investigated by Jager-Contreras (1977) who reported the precise location of the mineralized bodies and described their morphology, size and field relations, but did not provide chemical data. Kuipjers and Jager-Contreras (1979) reported bulk chromium contents ranging from 33.1 to 61.0wt% Cr_2O_3 in 21 samples (average: 48.5wt% Cr_2O_3). Based on structural considerations, the authors concluded that the chromitites were produced by fractional crystallization of a basic magma migrating through the peridotite. This study documents the results of the first systematic investigation of chromite composition by electron-microprobe in the chromitites of Santa Elena, and provides the first data on the distribution and mineralogy of PGE within chromite grains. The data are used to identify the petrogenetic nature of the parental melt of the chromitites and, indirectly, define the tectonic setting of their emplacement. The role of the chromitites as a petrogenetic indicator represents a new approach that may contribute to resolving the geodynamic puzzle of the Santa Elena Ultramafic Nappe.

GEOLOGICAL BACKGROUND AND DESCRIPTION OF THE CHROMITITES

The Santa Elena mafic-ultramafic complex constitutes a large part of the rock exposed along the Santa Elena Peninsula on the northern Pacific coast of Costa Rica, close to the border with Nicaragua (Fig. 1B). According to Tournon (1994) and Baumgartner et al. (2008), Santa Elena Peninsula consists of three major structural units: 1) an overthrust allochthonuos unit composed of mafic-ultramafic rocks (Santa Elena Nappe), 2) a Cretaceous igneous-sedimentary sequence resting immediately below the overthrust (Santa Rosa Accretionary Complex), and 3) a volcanic sequence of pillow and massive basalts (Islas Murciélago) with IAT-affinity and $^{40}Ar/^{39}Ar$ age of 109Ma (Hauff et al., 2000). The Santa Elena Nappe is a regional SW-verging thrust over the Santa Rosa

accretionary complex (Tournon, 1994). The ultramafic rocks are composed of partially to completely serpentinized peridotite, mostly diopside-bearing harzburgite, with minor plagioclase lherzolite, dunite and orthopyroxenite. Layered gabbros and plagiogranite bodies occur along the southeastern coast, whereas dikes of pegmatitic gabbro and dolerite cut across the peridotite along its northern boundary (Gazel et al., 2006; Denyer and Gazel, 2009). The age of radiolarian cherts of the Santa Rosa accretionary complex varies from Middle Jurassic to Lower Cretaceous,
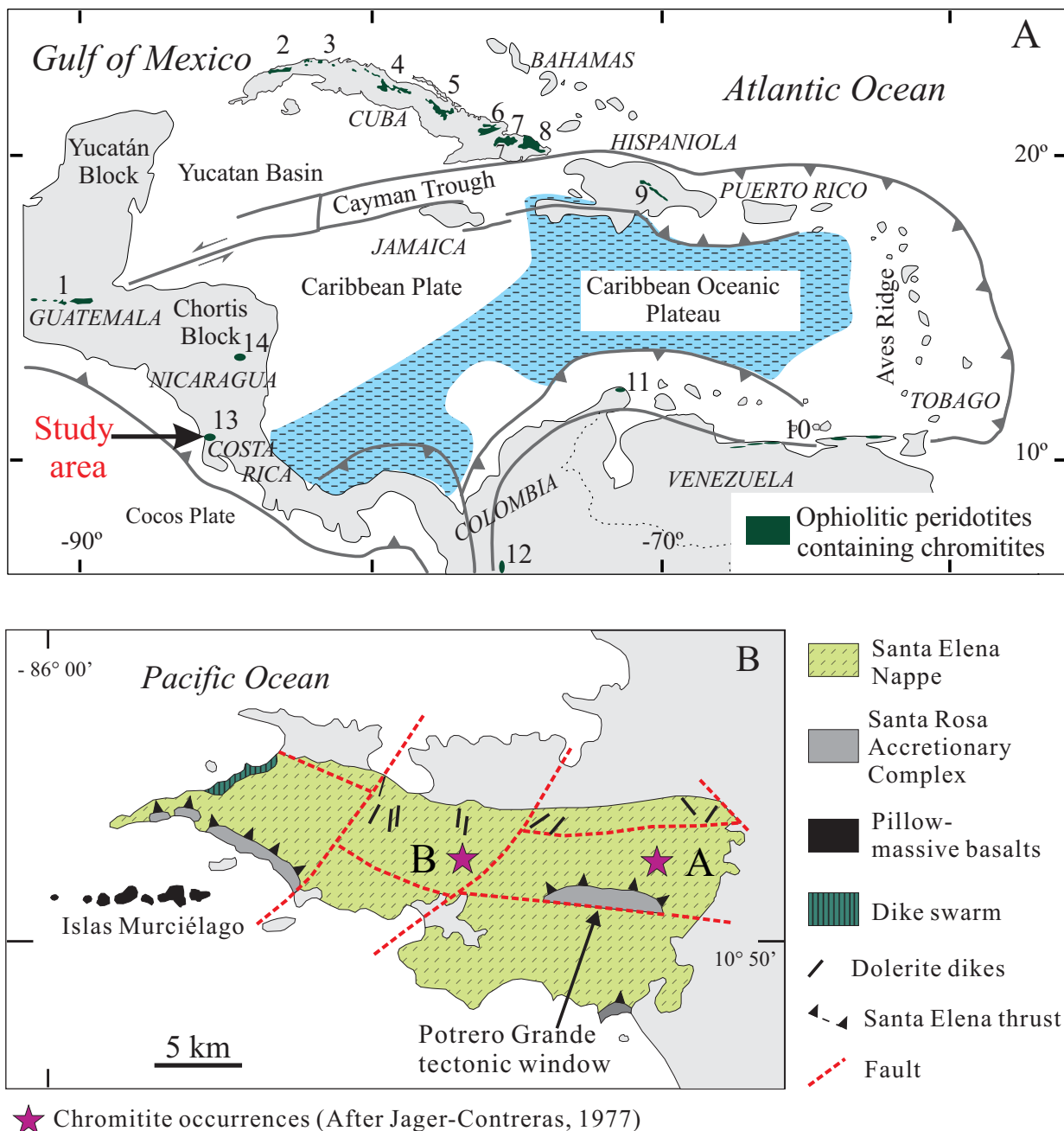

FIGURE 1 | A) Structural sketch map showing distribution of ophiolite complexes with peridotite-host chromitite along the margin of the Caribbean plate. Locality number; 1: *Baja Verapaz*, Guatemala (Thayer, 1946); 2. to 8: *Cajálbana, Habana-Matanza, Villa Clara, Camagüey, Holguín, Mayarí-Cristal, Moa-Baracoa*, Cuba (Thayer, 1946; Proenza and Melgarejo, 1998; Proenza et al., 1999); 9: *Loma Caribe*, Dominican Republic (Proenza et al., 2007; Zaccarini et al., 2009); 10: *La Franja Costera*, Venezuela (Thayer, 1946; Rodriguez, 1986); 11: *La Guajira*, 12: *Dunita de Medellin*, Colombia (Álvarez, 1987; Buenaventura, 2001; Proenza et al., 2004); 13: *Santa Elena*, Costa Rica (Jager-Contreras, 1977; Kuipjers and Jager-Contreras, 1979; this study); 14: *Siuna*, Nicaragua (Flores et al., 2007; Baumgartner et al., 2008). B) Geological sketch map of the Santa Elena peninsula showing location of two chromitite areas (A and B) after Jager-Contreras (1977). Only chromitites from area A were investigated in this study.

suggesting that the oceanic assemblage beneath the Santa Elena Nappe represents a discontinuous stratigraphic sequence (Baumgartner and Denyer, 2006; Baumgartner et al., 2008).

Eight chromitite bodies have been reported by Jager-Contreras (1977) and Kuipjers and Jager-Contreras (1979), occurring in two separated areas (A and B) along the central axis of the Santa Elena ultramafic body (Fig. 1B). Area A is located some kilometers north of the Potrero Grande tectonic window, and covers a surface of about 2km². The ore bodies occur a few ten to a few tens of meters to a few hundred off the old track leading to Cerro El Inglés. Area B is located in a remote, mountainous region currently inaccessible. Therefore only the six chromitite occurrences located in area A were sampled and studied in this work. Samples have been labeled from Jag-1 to Jag-6 according with the numeration of Jager-Contreras (1977) (Fig. 2), and are listed in Table 1 along with GPS coordinates. At the outcrop scale, the chromitites are small and irregular bodies (Figs. 3, 4) with a predominantly massive texture that locally grades into orbicular or leopard texture. It was not possible to recognize the lithology of the host ultramafic rock, in most cases, due to strong alteration. However, some of the chromitite bodies are in direct contact with partially altered dunite. Small patches of relatively fresh clinopyroxenite and gabbro (possibly dikes) occur in the peridotites from area A, away from the chromitite bodies.

ANALYTICAL TECHNIQUES

A total number of 24 polished sections (4 from each one of the six chromitite occurrences) were examined. Chromite and PGM were analyzed by electron microprobe with a Superprobe Jeol JXA 8200 at the Eugen F. Stumpfl Laboratory at Leoben University. Back scattered electron (BSE) images of the PGM were obtained at the Leoben laboratory as well as at the Serveis Cientificotècnics at the Universitat de Barcelona. Eleven samples of massive chromitite and two of peridotites were analyzed for PGE and Au by Inductively Coupled Plasma-Mass Spectrometry (ICP-MS) after Ni-sulfide preconcentration at Genalysis Laboratory Services Pty Ltd, Western Australia.

In order to determine the primary composition of chromite, care was taken to analyze the unaltered cores of grains. An average of 20 analysis points were obtained for each polished section. The electron microprobe was operated in the Wavelength Dispersive X-Ray Spectrometry (WDS) mode, at 15kV accelerating voltage and10nA beam current. The analysis of Mg, Al, Ti, V, Cr, Mn, Fe, Ni and Zn were carried out using the Kα lines, and were calibrated on natural chromite, rhodhonite, ilmenite and metallic V, Ni and Zn. The counting times for peak and background
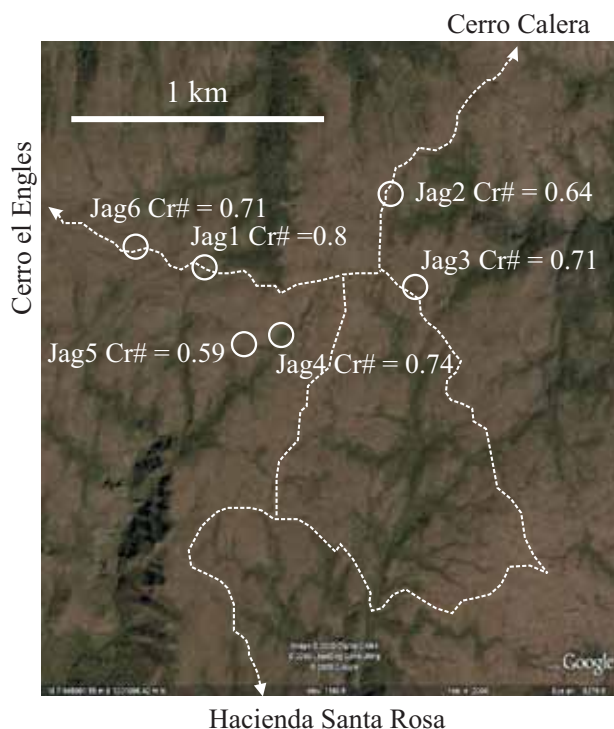

FIGURE 2 | **Google satellite view of area A with spatial distribution of the six chromitite localities investigated. Average chromium numbers, Cr#=Cr/(Cr+Al), in each chromite locality are shown (see text for discussion).**

were 20 and 10 seconds respectively. The amount of Fe^{3+} in chromite was calculated assuming the spinel stoichiometry $R^{2+}O\ R^{3+}_2O_3$.

PGM were previously located by scanning polished sections under a reflected light microscope at 250-800 magnification. They were subsequently analyzed on the Electron Probe Microanalyzer in the WDS mode, at 20kV accelerating voltage and 10nA beam current, and beam diameter of about 1 micron or less. The counting time on peak and background were 15 and 5 seconds respectively. The Kα lines were used for S, As, Fe, Cu and Ni; Lα for Ir, Ru, Rh and Pt, and Mα for Os. The reference materials

TABLE 1 | **GPS coordinates of the investigated chromities from locality A, samples Jag 1-6 (Fig. 1).**

Jag 1	85°40'10.50"W	10°52'26.00"N
Jag 2	85°39'44.60"W	10°52'32.30"N
Jag 3	85°39'40.30"W	10°52'22.20"N
Jag 4	85°39'52.20"W	10°52'18.20"N
Jag 5	85°39'55.60"W	10°52'17.00"N
Jag 6	85°40'21.40"W	10°52'28.80"N

were pure metals for the six PGE (Ru, Rh, Pd, Os, Ir, Pt), synthetic NiS, natural chalcopyrite and niccolite for Ni, Fe, Cu, S and As. The following diffracting crystals were selected: PETJ for S; PETH for Ru, Os, Rh; LIF for Cu; LIFH for Ni, Ir, Pt; and TAP for As. Automatic corrections were performed for interferences involving Ru-Rh, Ir-Cu and Rh-Pd.

RESULTS

Chromite texture and composition

Under the microscope, the chromitites of Santa Elena display a uniform massive texture (<10% interstitial silicate) interrupted by cracks, pull-apart fractures and brecciation (Fig. 5A). Chromite is usually fresh, showing the typical ferrian-chromite alteration only along grain boundaries and cracks (Fig. 5B).

Approximately 500 electron microprobe analyses were performed on 15 samples from the six chromitite occurrences, and are listed as averages in Table 2. Chromites are compositionally homogeneous or display little variation within single localities. However, substantial differences are seen from one locality to the other. The overall variation ranges of major oxides
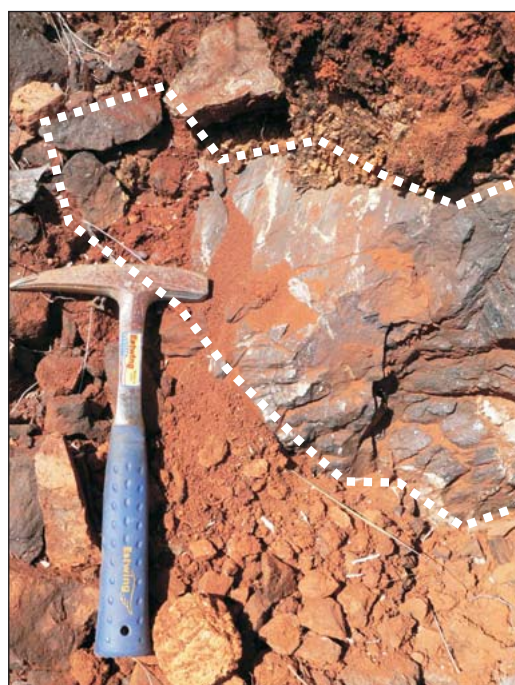

FIGURE 3 | **Field photographs of the massive chromitite and strongly lateritized peridotite host at locality Jag-1.**
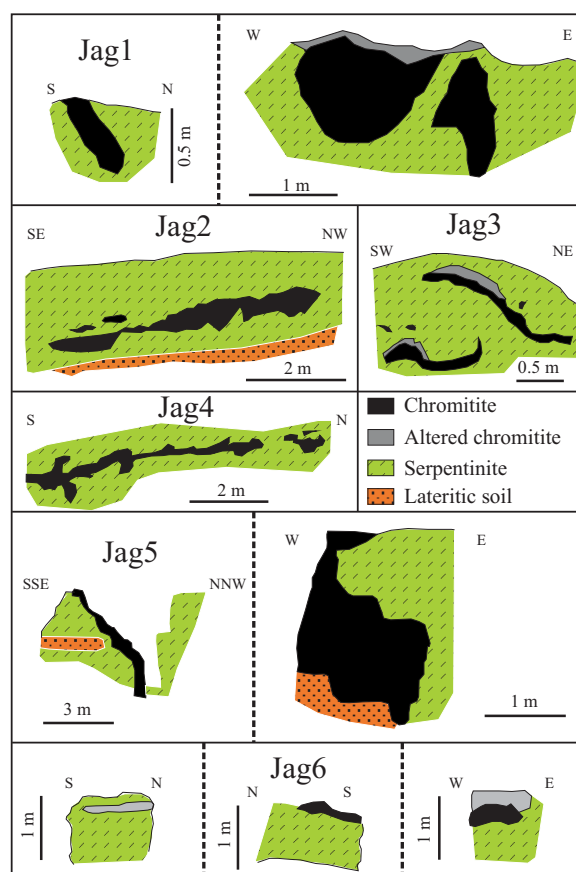

FIGURE 4 | **Oriented field sketches of chromitite bodies at the six localities in area A (redrawn and simplified after Jager-Contreras, 1977).**

(wt%) in the unaltered cores of chromite grains are: Cr_2O_3 (42.8-62.75), Al_2O_3 (7.1-24.5), MgO (9.3-14.0) and FeO (13.2-20.6). MgO and FeO display negative correlation (R=-0.76). A sharp negative correlation (R=-0.98) is also observed between Cr_2O_3 and Al_2O_3 (Fig 6A), consistent with the Al-Cr substitution predominant in podiform chromitites compared with the stratiform type (Thayer, 1970). The TiO_2 content varies between 0.1wt% and 0.35wt%, showing a well defined negative correlation with Cr_2O_3 (R=-0.91) (Fig. 6B), and positive with Al_2O_3 (R=0.88).

The calculated amount of Fe_2O_3 is usually low (<1.75wt%) and near zero in samples Jag-1 and Jag-4, which have the highest Cr contents. Maximum concentrations of 0.29wt% NiO (av.=0.05-0.19), 0.23wt% ZnO (av.=0.03-0.10), and 0.14wt% V_2O_3 (av.=0.04-0.09) have been
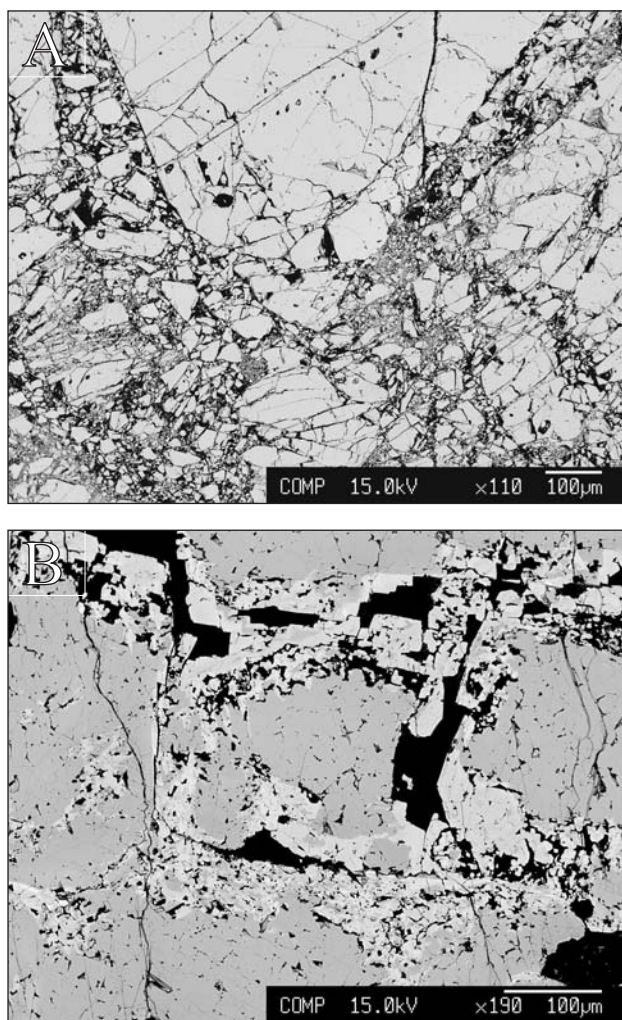

FIGURE 5 | **Back scattered electron images of polished sections from the Santa Elena chromitites. A) Coarse grained chromitite with strong brecciation controlled by shear planes. B) Ferrian chromite alteration (light grey) developed along cracks and fissures in massive chromitite.**

determined. The Mn content is lower than 0.15wt% MnO, and typically below the detection limit.

Santa Elena chromitites plot in the podiform field on the Cr/(Cr+Al) vs. $Fe^{2+}/(Fe^{2+}+Mg)$ binary diagram (Fig. 6C). The compositions from the various localities form a continuous trend from extremely chromiferous (av. Cr/(Cr+Al)=0.81), to intermediate and aluminous (av. Cr/(Cr+Al)=0.54), in a relatively narrow variation range in $Fe^{2+}/(Fe^{2+}+Mg)$ (0.52-0.38).

Chemical effects of alteration in Santa Elena chromitites are rather unusual compared with common chemical patterns observed in hydrothermally altered chromitites. Altered rims exhibit a consistent decrease in Al and an irregular decrease in all other analyzed elements, except Fe^{2+} and Cr that are variably enriched. Thus, the expected oxidation of Fe^{2+} to Fe^{3+} is not observed. On the contrary, a general sharp drop of Fe^{3+} occurs in the alteration rims with respect to the cores. A similar alteration pattern has been described in detrital chromian spinels from lateritic soils formed by tropical weathering of ultramafic rocks (Friedrich et al., 1980).

PGE geochemistry and mineralogy

Total PGE concentration in 11 chromitite samples ranges from 80 to 292ppb and is about 4 to 10 times higher than in serpentinized peridotites (Table 3). There is no obvious correlation between PGE abundance and chromite composition. We note, however, that the highest PGE concentrations and the lowest Pd/Ir ratios were found in the most Cr-rich chromitite from Jag-1 locality. All samples display enrichment in Ru (48-183ppb), Ir (17-81ppb) and Os (12-69ppb), with good positive correlation among the pairs Os-Ir (R^2=0.90), Ir-Ru (R^2=0.93), Os-Ru (R^2=0.88). Rh and Pd contents range from 7 to 18ppb and 3 to 5ppb, respectively. Gold and Pt are always below the detection limit, except for samples from Jag-1, which contain 3 ppb Pt.

Chondrite-normalised PGE patterns of Santa Elena chromitites display high (Os+Ir+Ru)/(Rh+Pt+Pd) ratios typical of Cr-rich chromitites formed in the mantle section of supra subduction zone ophiolites of the Balkan Peninsula (Economou-Eliopoulos, 1996; Kocks et al., 2007), Turkey (Uysal et al., 2009a, b), Urals (Melcher et al., 1997; Garuti et al., 2005), Caribbean Belt (Proenza et al., 1999), and China (Zhou et al., 1998). In most cases, PGE patterns are characterized by a consistent positive anomaly in Ru, and a negative anomaly in Pt (Fig. 7A, B). The chondrite-normalized pattern of serpentinized peridotite of Santa Elena is shifted to one order of magnitude less compared with the chromitites. However, the peridotite patterns are generally flat and have Ru and Pt anomalies

TABLE 2 | **Average compositions of chromite and calculated parental melts from 6 chromitite occurrences in the Santa Elena peridotite**

Weight % (normalized to 100%)													
Locality-Sample	N°an.	TiO_2	Al_2O_3	FeO	Fe_2O_3	MgO	MnO	Cr_2O_3	NiO	ZnO	V_2O_3	$*Al_2O_3$	$*TiO_2$
Chromite core													
Jag1-1	15	0.14	10.21	15.36	0.08	11.73	0.00	62.27	0.08	0.06	0.06	11.02	0.30
Jag1-2	18	0.12	10.36	14.67	0.00	12.09	0.03	62.48	0.13	0.05	0.07	11.09	0.26
Jag1-2 BC	20	0.12	11.60	15.48	0.00	11.62	0.05	60.91	0.11	0.05	0.06	11.68	0.26
Jag1-3	20	0.13	10.32	14.82	0.00	11.81	0.00	62.67	0.14	0.04	0.06	11.07	0.28
Jag2-1	20	0.29	18.89	15.41	0.64	12.85	0.07	51.55	0.16	0.06	0.08	14.23	0.45
Jag2-2	34	0.29	19.42	16.27	0.81	12.34	0.09	50.48	0.16	0.06	0.08	14.37	0.46
Jag2-2 BC	20	0.21	18.15	19.02	1.63	10.33	0.12	50.31	0.11	0.07	0.06	14.02	0.39
Jag2-3	20	0.31	19.49	15.43	0.97	12.88	0.12	50.48	0.19	0.05	0.07	14.39	0.47
Jag3-1	20	0.23	15.95	16.37	0.80	11.94	0.00	54.46	0.11	0.06	0.08	13.34	0.41
Jag3-1 BC	20	0.20	15.83	16.40	1.10	11.84	0.09	54.34	0.13	0.07	0.00	13.30	0.37
Jag3-2	20	0.20	14.52	17.57	1.16	10.97	0.07	55.27	0.10	0.06	0.09	12.85	0.38
Jag3-2 BC	20	0.20	15.45	18.11	1.68	10.67	0.09	53.59	0.09	0.05	0.06	13.18	0.38
Jag4-2	20	0.18	13.27	15.94	0.01	11.72	0.16	58.47	0.12	0.07	0.07	12.38	0.35
Jag4-2 BC	20	0.20	17.55	19.47	0.29	9.93	0.13	52.21	0.07	0.10	0.06	13.84	0.38
Jag4-3	30	0.19	13.68	17.07	0.43	11.20	0.12	57.09	0.10	0.05	0.07	12.54	0.37
Jag5-1	20	0.33	21.19	15.88	0.24	12.83	0.06	49.20	0.12	0.06	0.09	14.83	0.48
Jag5-2	20	0.35	23.64	15.15	0.65	13.56	0.06	46.31	0.13	0.07	0.09	15.40	0.49
Jag5-2 BC	20	0.30	22.35	17.53	1.33	11.45	0.04	46.82	0.10	0.08	0.02	15.10	0.47
Jag5-3	20	0.32	21.09	15.78	0.18	12.86	0.06	49.44	0.12	0.07	0.09	14.80	0.47
Jag6-2	30	0.20	14.96	18.96	1.05	10.11	0.08	54.41	0.07	0.10	0.07	13.01	0.38
Jag6-3	20	0.20	13.70	19.17	0.96	9.85	0.08	55.83	0.06	0.08	0.07	12.55	0.37
Altered chromite rim													
Jag1-1	6	0.10	6.82	15.92	0.00	10.36	0.00	66.66	0.06	0.03	0.04		
Jag1-2	2	0.13	10.45	14.57	0.00	12.03	0.03	62.58	0.07	0.08	0.07		
Jag2-2	26	0.16	14.71	19.11	0.99	9.99	0.04	54.79	0.06	0.06	0.09		
Jag1-3	20	0.12	6.85	15.66	0.00	10.01	0.04	67.14	0.06	0.05	0.07		

Atomic% (based on 32 Oxygens)												
Locality-Sample	Ti	Al	Fe^{2+}	Fe^{3+}	Mg	Mn	Cr	Ni	Zn	V	#Cr	$\#Fe^{2+}$
Chromite core												
Jag1-1	0.03	3.15	3.36	0.02	4.57	0.00	12.86	0.02	0.01	0.01	0.80	0.42
Jag1-2	0.02	3.55	3.36	0.00	4.50	0.01	12.51	0.02	0.01	0.01	0.78	0.43
Jag1-2 BC	0.02	3.18	3.20	0.00	4.69	0.01	12.87	0.03	0.01	0.01	0.80	0.41
Jag1-3	0.02	3.18	3.24	0.00	4.59	0.00	12.93	0.03	0.01	0.01	0.80	0.41
Jag2-1	0.05	5.57	3.22	0.12	4.79	0.02	10.19	0.03	0.01	0.01	0.65	0.40
Jag2-2	0.06	5.73	3.41	0.15	4.60	0.02	9.99	0.03	0.01	0.01	0.64	0.43
Jag2-2 BC	0.04	5.46	4.06	0.31	3.93	0.03	10.15	0.02	0.01	0.01	0.65	0.51
Jag2-3	0.06	5.73	3.22	0.18	4.79	0.03	9.95	0.04	0.01	0.01	0.63	0.40
Jag3-1	0.05	4.79	3.49	0.15	4.53	0.00	10.96	0.02	0.01	0.01	0.70	0.44
Jag3-1 BC	0.04	4.76	3.50	0.21	4.50	0.02	10.95	0.03	0.01	0.00	0.70	0.44
Jag3-2	0.04	4.41	3.79	0.23	4.22	0.02	11.27	0.02	0.01	0.01	0.72	0.47
Jag3-2 BC	0.04	4.69	3.90	0.33	4.09	0.02	10.91	0.02	0.01	0.01	0.70	0.49
Jag4-2	0.04	4.03	3.44	0.00	4.50	0.04	11.92	0.02	0.01	0.01	0.75	0.43
Jag4-2 BC	0.04	5.30	4.17	0.06	3.79	0.03	10.58	0.01	0.02	0.01	0.67	0.52
Jag4-3	0.04	4.17	3.69	0.08	4.31	0.03	11.66	0.02	0.01	0.01	0.74	0.46
Jag5-1	0.06	6.19	3.28	0.04	4.73	0.01	9.64	0.02	0.01	0.01	0.61	0.41
Jag5-2	0.06	6.80	3.09	0.12	4.93	0.01	8.94	0.03	0.01	0.01	0.57	0.39
Jag5-2 BC	0.06	6.55	3.65	0.25	4.24	0.01	9.21	0.02	0.01	0.00	0.58	0.46
Jag5-3	0.06	6.16	3.27	0.03	4.75	0.01	9.68	0.02	0.01	0.01	0.61	0.41
Jag6-2	0.04	4.57	4.10	0.21	3.90	0.02	11.14	0.01	0.02	0.01	0.71	0.51
Jag6-3	0.04	4.21	4.18	0.19	3.83	0.02	11.51	0.01	0.02	0.01	0.73	0.52
Altered chromite rim												
Jag1-1	0.02	2.15	3.57	0.00	4.13	0.00	14.11	0.01	0.01	0.01	0.87	0.46
Jag1-2	0.03	3.21	3.17	0.00	4.67	0.01	12.89	0.01	0.02	0.01	0.80	0.40
Jag2-2	0.02	2.17	3.52	0.00	4.01	0.01	14.25	0.01	0.01	0.01	0.87	0.47
Jag1-3	0.03	4.50	4.15	0.19	3.86	0.01	11.24	0.01	0.01	0.01	0.71	0.52

N°an. = number of analyses; $*TiO_2$ and $*Al_2O_3$ = calculated Silicate melt in equilibrium with chromite (see equations in Fig. 11)

#Cr = Cr/(Cr+Al)

$\#Fe^{2+} = Fe^{2+}/(Fe^{2+}+Mg)$
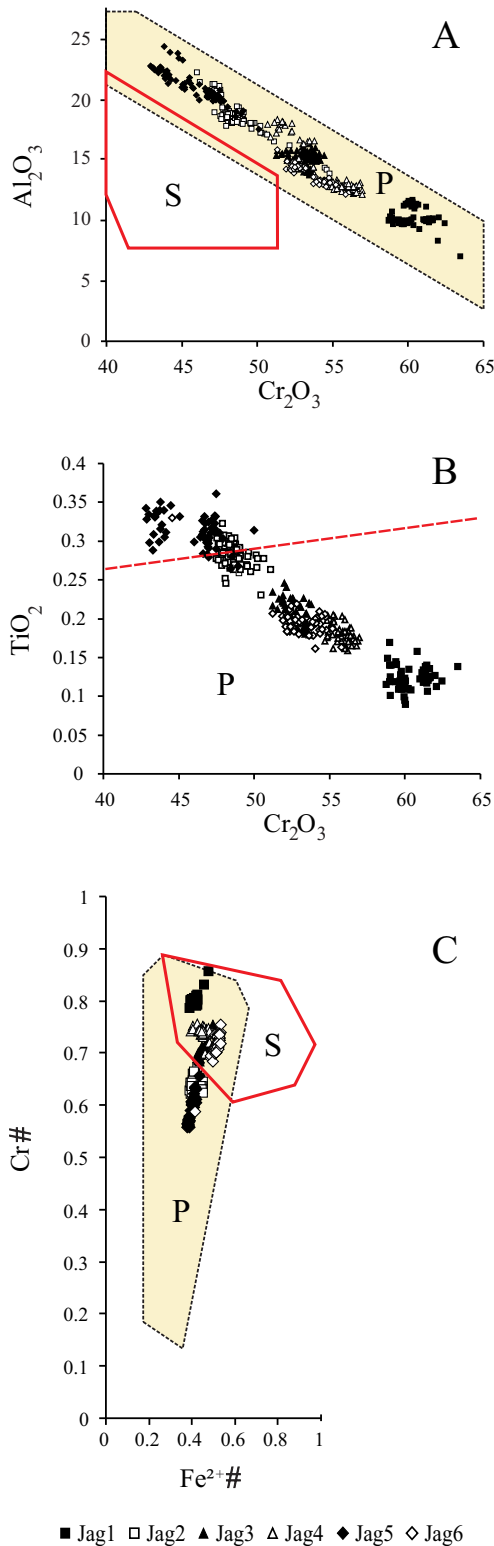
■ Jag1   □ Jag2   ▲ Jag3   △ Jag4   ◆ Jag5   ◇ Jag6

FIGURE 6 | **Composition of unaltered chromite cores in chromite from the six chromitite localities (area A) of Santa Elena. A and B) Sharp negative correlation of Al_2O_3 and TiO_2 versus Cr_2O_3. C) variation of the chromium number, $Cr\#=Cr/(Cr+Al)$, as a function of the bivalent iron number, $Fe^{2+}\#=Fe^{2+}/(Fe^{2+}+Mg)$. P: field of podiform chromitites, S: field of stratiform chromitites.**

TABLE 3 | **Concentration of PGE and Au (ppb) in the Santa Elena chromitite and serpentinite**

	Os	Ir	Ru	Rh	Pt	Pd	Au	ΣPGE
d.l.	2	2	2	2	2	2	5	
Chromitite								
JAG 1-1	69	81	183	16	3	4	b.d.l.	287
JAG 1-1	68	81	180	17	3	5	b.d.l.	286
JAG 1-3	69	85	181	18	3	5	b.d.l.	292
JAG 2-1	38	32	95	9	b.d.l.	4	b.d.l.	140
JAG 3-3	12	17	48	10	b.d.l.	5	b.d.l.	80
JAG 4-1	30	41	135	14	b.d.l.	4	b.d.l.	194
JAG 4-2	15	25	79	12	b.d.l.	4	b.d.l.	120
JAG 4-3	19	30	98	12	b.d.l.	4	b.d.l.	144
JAG 5-2	42	40	119	7	b.d.l.	3	b.d.l.	169
JAG 5-3	54	48	154	8	b.d.l.	4	b.d.l.	214
JAG 6-3	17	26	48	9	b.d.l.	4	b.d.l.	87
Serpentinite								
MV-2	5	5	10	2	6	9	b.d.l.	32
MV-3	4	4	8	b.d.l.	3	6	b.d.l.	21
CC1	514	540	690	200	1020	545		

d.l. = detection limit, b.d.l. = below detection limit,
CC1 = chondrite values after Naldrett and Duke (1980)

similar to those of the chromitites, although the Pt+Pd contents are higher (Fig. 7A).

The mineralogical study of 24 polished sections resulted in finding 50 PGM grains, with a minimum frequency of at least one grain per section. The mineralogy reflects the chemical data, showing relative abundance of Ru, Ir and Os minerals, and absence of distinct Rh, Pt and Pd phases. The most abundant PGM is laurite (RuS_2), accompanied by minor erlichmanite (OsS_2) and irarsite (IrAsS). Native Os and other unidentified PGE-sulfides (Ir-Rh-S, Ir-Ni-Fe-Cu-S, Ir-Os-Ru-As-S) were also observed. Microprobe analyses (Table 4) show that minor amounts of Rh and Pd and variable amounts of Ni, Fe and Cu are carried in laurite and erlichmanite. Minor but consistent amounts of As substitute for S. Distinct arsenic minerals (i.e. irarsite) were identified, but could not be quantitatively analyzed because of their small grain size. These PGM are usually less than $10\mu m$ in size. They are euhedral and occur as inclusions either in fresh chromite (Fig. 8A, B) or in ferrian chromite (Fig. 8E), locally in contact with fractures (Fig. 8D). More rarely, they are found in a chlorite matrix filling cracks in the massive chromite (Fig. 8C). Most of the PGM form single phase grains, however some form composite inclusions with primary silicates (clinopyroxene, amphibole), or occur associated with secondary minerals (chlorite, Ni-sulfides, chalcopyrite) in the altered matrix of the chromitites. Native Os was only qualitatively identified. It was found as minute particles ($<1\mu m$ in size) attached to the external border of laurite (Fig. 8E), or enclosed within NiS-CuS composite grains (Fig. 8F), the texture suggesting that osmium is a low-temperature exsolution product from laurite.

Sulfides of the laurite-erlichmanite series do not show significant compositional variations in relation to their textural association with primary magmatic (chromite, clinopyroxene, amphibole) or secondary alteration minerals (ferrian chromite, chlorite), as is common for altered laurite (Zaccarini et al., 2005). On the contrary, they have similar Ru-Os-Ir relationships regardless of their paragenetic association (Fig. 9).

DISCUSSION

Origin of chromite compositional variations at Santa Elena

Major compositional variations of chromite in Santa Elena chromitites involve sharp negative correlations of Al and Ti vs. Cr, and illustrate continuous trends between Cr-rich/Ti-poor and Al-rich/Ti-rich compositional end members.

According to theoretical predictions (Maurel and Maurel, 1982), high-Cr chromite crystallizes from less aluminous melts (picritic or boninitic basalts) than high-Al chromite (normal MORB). The coexistence of Al-rich and Cr-rich chromitites within the same ophiolite complex has been observed worldwide (e.g. Leblanc and Nicolas, 1992; Zhou and Bai, 1992; Leblanc, 1995; Melcher et al., 1997; Proenza et al., 1999; Savelieva, 2004; Kocks et

al., 2007; Rollinson, 2008; Uysal et al., 2007; 2009b). In places, a clear bimodal distribution and vertical zoning are observed (Leblanc and Nicolas, 1992), the Cr-rich type being located in the deep mantle section, and the Al-rich type occurring higher in the stratigraphy, close to the Moho transition, with stratigraphic distances not less than 1-2km. This may reflect: 1) separate intrusions of magmas derived from differently depleted mantle sources (e.g.: MORB vs. boninite), during regression of the oceanic lithosphere from the MOR towards supra subduction zone regions; 2) mixing of different magmas produced by multi-stage melting of a partially re-fertilized and fluid-metasomatized residual source, in supra subduction zone regions; 3) reaction of a single parental melt (boninitic) with country-rock peridotites having variable residual character; 4) fractional precipitation during differentiation of a single melt with initial high-Cr boninitic composition in supra subduction zone regions. All mechanisms require quite a large space-time gap for the formation of Al-rich and Cr-rich chromitites coexisting within the same mantle, except for mechanism 4, which can occur in relatively short times and narrow spaces.

At Santa Elena, Cr and Al-rich chromitites occur in close vicinity, not separated by relevant faults, with estimated distances of less than 100 meters. The continuous variation from the Cr-rich to intermediate and aluminous compositions is interpreted as due to the fractionation of
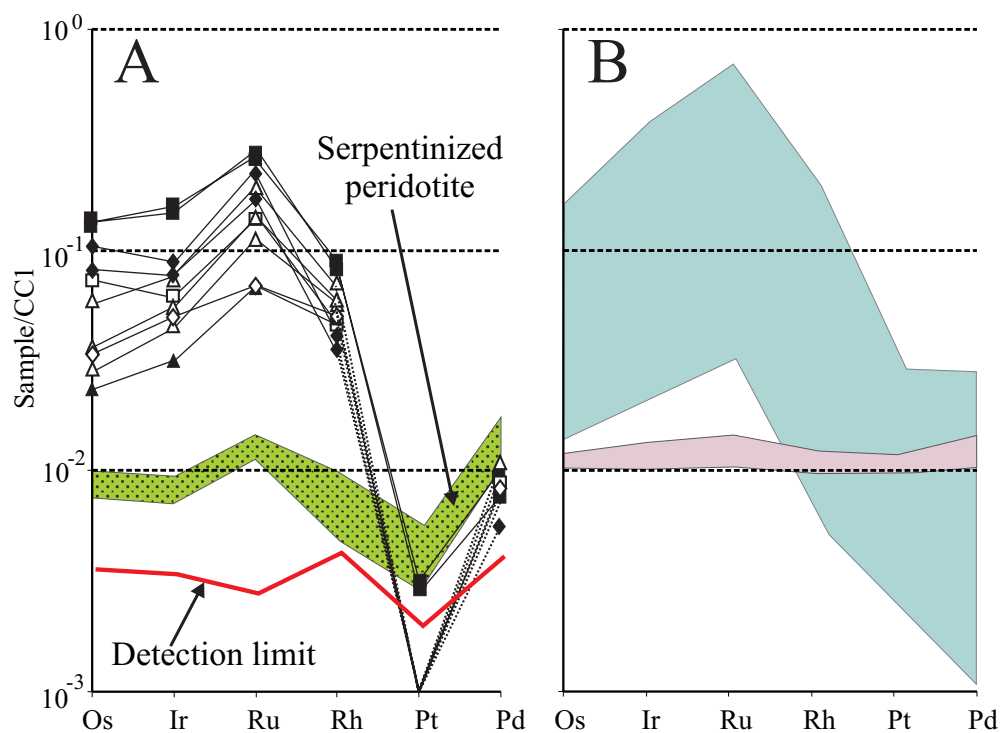

FIGURE 7 | A) Chondrite-normalized patterns of chromitite and partially altered peridotite (dotted green area) from Santa Elena; normalization values from Naldrett and Duke (1980) are shown in Table 3. B) PGE chondritic patterns for Cr-rich ophiolitic chromitite from supra subduction zone setting (blue field) and host peridotite (purple field). Data source include: Economou-Eliopoulos (1996), Kocks et al. (2007), Uysal et al. (2007; 2009a, b), Melcher et al. (1998), Garuti et al. (2005), Proenza et al. (1999), and Zhou et al. (1998).

TABLE 4 | **Representative composition of minerals of laurite-erlichmanite series in the Santa Elena chromitites**

Wt%	Os	Ir	Ru	Rh	Pt	Pd	S	As	Cu	Fe	Ni	Total
d.l.	0.8	0.1	0.02	0.01	0.1	0.02	0.01	0.05	0.04	0.02	0.04	
Enclosed in chromite												
jag2-2-3-1	2.16	9.39	43.26	3.15	b.d.l.	2.77	35.13	3.12	0.40	0.97	0.58	100.93
jag5-1-4-1	26.32	4.59	28.58	0.67	b.d.l.	1.45	32.83	1.19	0.07	2.06	2.07	99.83
jag5-2-2-3	23.61	7.40	30.92	0.65	b.d.l.	1.53	32.46	1.21	0.11	1.28	0.25	99.42
jag6-1-2-1	23.00	1.57	37.27	0.83	b.d.l.	1.88	34.20	1.47	0.13	0.80	0.13	101.28
jag6-1-2-2	22.09	1.90	37.48	0.79	b.d.l.	1.87	34.62	1.45	0.05	0.73	0.06	101.04
In contact with chlorite and ferrian chromite												
jag1-1-1-1	13.24	5.84	39.99	1.79	b.d.l.	2.12	34.11	1.68	0.04	0.78	0.15	99.74
jag4-2-2-1	10.87	4.38	41.41	4.18	b.d.l.	3.10	35.15	2.03	0.10	0.71	0.11	102.04
jag4-2-2-2	12.27	4.45	40.20	3.95	b.d.l.	2.99	34.38	1.84	0.06	0.91	0.14	101.19
jag6-3-5-1	46.47	4.28	16.13	0.59	b.d.l.	0.79	28.63	0.61	0.06	0.99	0.08	98.63
jag6-3-5-2	20.77	3.72	35.98	1.95	b.d.l.	2.09	31.16	1.75	0.09	0.92	0.06	98.49
jag1-1-3-1	20.38	10.28	30.33	1.76	b.d.l.	1.70	32.51	1.57	0.16	0.56	0.16	99.41
jag2-1-2a-1	17.14	9.04	34.19	2.27	b.d.l.	2.48	33.47	1.96	0.12	0.41	0.13	101.21
jag6-1-3-1	13.31	1.96	45.45	1.14	b.d.l.	2.35	35.82	1.85	b.d.l.	0.53	b.d.l.	102.41
jag6-1-3-2	13.03	2.13	45.45	1.12	b.d.l.	2.39	35.64	1.77	b.d.l.	0.52	0.07	102.12
jag6-1-3-3	15.98	1.60	42.80	1.11	b.d.l.	2.16	34.56	1.81	b.d.l.	0.52	0.08	100.62
At%	Os	Ir	Ru	Rh	Pt	Pd	S	As	Cu	Fe	Ni	
Enclosed in chromite												
jag2-2-3-1	0.66	2.85	24.95	1.78	b.d.l.	1.52	63.87	2.42	0.36	1.01	0.58	
jag5-1-4-1	8.77	1.51	17.92	0.41	b.d.l.	0.86	64.88	1.01	0.07	2.34	2.23	
jag5-2-2-3	8.03	2.49	19.78	0.41	b.d.l.	0.93	65.45	1.05	0.11	1.48	0.28	
jag6-1-2-1	7.43	0.50	22.65	0.49	b.d.l.	1.09	65.51	1.21	0.12	0.88	0.14	
jag6-1-2-2	7.10	0.60	22.67	0.47	b.d.l.	1.07	66.00	1.18	0.05	0.80	0.06	
In contact with chlorite and ferrian chromite												
jag1-1-1-1	4.25	1.86	24.18	1.06	b.d.l.	1.22	65.01	1.37	0.04	0.85	0.15	
jag4-2-2-1	3.36	1.34	24.12	2.39	b.d.l.	1.72	64.53	1.59	0.09	0.74	0.11	
jag4-2-2-2	3.87	1.39	23.84	2.30	b.d.l.	1.68	64.27	1.47	0.05	0.97	0.15	
jag6-3-5-1	17.96	1.64	11.73	0.42	b.d.l.	0.54	65.63	0.60	0.07	1.30	0.10	
jag6-3-5-2	7.15	1.27	22.68	1.24	b.d.l.	1.29	63.61	1.53	0.09	1.08	0.07	
jag1-1-3-1	6.94	3.46	19.44	1.11	b.d.l.	1.03	65.67	1.36	0.16	0.65	0.17	
jag2-1-2a-1	5.62	2.94	21.11	1.38	b.d.l.	1.45	65.15	1.63	0.11	0.46	0.14	
jag6-1-3-1	4.08	0.59	26.23	0.65	b.d.l.	1.29	65.16	1.44	b.d.l.	0.56	b.d.l.	
jag6-1-3-2	4.01	0.65	26.32	0.64	b.d.l.	1.31	65.07	1.38	b.d.l.	0.54	0.07	
jag6-1-3-3	5.06	0.50	25.51	0.65	b.d.l.	1.22	64.94	1.46	b.d.l.	0.56	0.08	

d.l. = detection limit, b.d.l. = below detection limit

a single batch of magma which was rapidly differentiating over short distances (mechanism 4). This model is further supported by the behavior of Ti. Santa Elena chromitites have a maximum Ti content similar to ophiolitic chromitites (<0.30wt% TiO_2, Dickey, 1975). However, Ti decreases continuously from the most aluminous samples down to the most Cr-rich ones, showing a sharp negative correlation with the Cr/Al ratio. This feature is not commonly observed in chromitite deposits of the Tethyan and Urals ophiolite belts. There, the Ti content may vary largely from Al-rich and Cr-rich chromitites, although the two types usually plot in separate fields without a clear differentiation trend (Zaccarini, 2005; Garuti et al., 2005).

Composition of the chromitite parental melt and geodynamic setting

The Cr/Al ratio in basaltic melts is a function of the degree of depletion of the mantle source, thus the ratio Cr/(Cr+Al) of chromite that crystallizes is an indirect reflection of the different geodynamic setting of magma formation (Irvine, 1967; Dick and Bullen, 1984; Roeder, 1994; Barnes and Roeder, 2001). Reciprocal variation of TiO_2 and Al_2O_3 in chromite helps to discriminate among spinels generated by MORB, OIB, and arc-related basaltic melts, as well as those from residual peridotite in supra subduction zone or MOR settings. Kamenestky et al. (2001) and Rollinson (2008) have shown that the
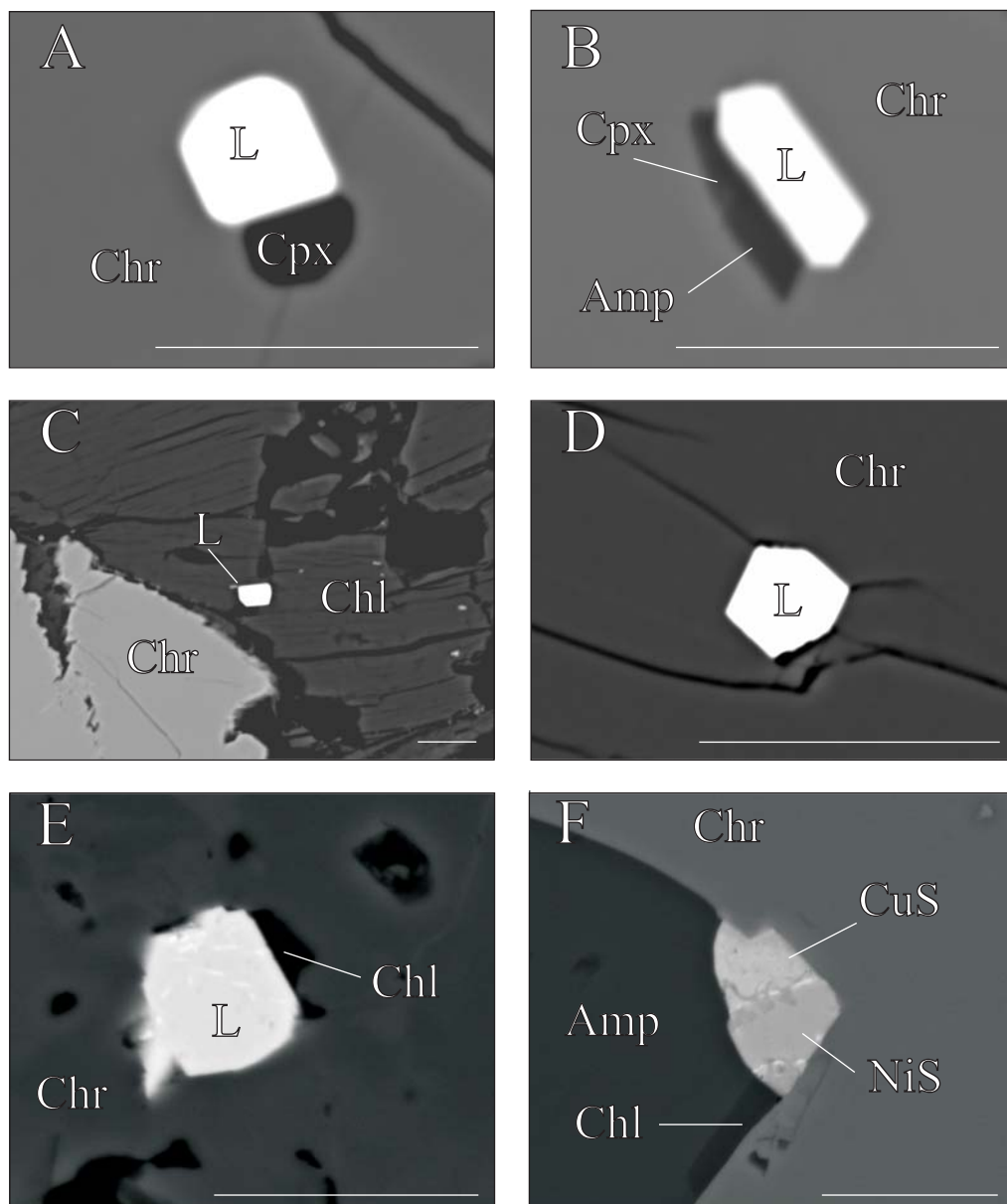
FIGURE 8 | **Back scattered electron images of Platinum-group minerals associated with the chromitites of Santa Elena. L: laurite (RuS$_2$). White spot visible in E and F are due to an Os bearing phase, possibly native Os. Scale bar = 10μm.**

array of MORB-type chromian spinel defines a roughly negative correlation trend in the TiO$_2$ vs. Al$_2$O$_3$ plot (Fig. 10). In contrast, Santa Elena chromites display a positive TiO$_2$-Al$_2$O$_3$ trend similar to spinels with an island arc basalt affinity and unequivocally fit the field of chromites from supra subduction zone residual peridotites, with only a few Ti- and Al-rich samples from the locality Jag-5 entering the MORB field (Fig. 10).

Using the approach of Rollinson (2008) and data from Kamenetsky et al. (2001), we have estimated the Al$_2$O$_3$ and TiO$_2$ contents of melts in equilibrium with the Santa Elena chromites (Table 2). Al$_2$O$_3$ and TiO$_2$

data for spinels and silicate melts from MOR and arc settings in Table 3 of Kamenetsky et al. (2001) were treated with the Excel Trend-Line software. They yielded best-fitting logarithmic expressions in all cases (R^2=0.68÷0.97), except for the TiO$_{2(melt)}$ vs. TiO$_{2(spinel)}$ in arc settings which show a linear regression line with R^2=0.91. When plotted on the regression lines, only samples from Jag-5 overlap the Al$_2$O$_3$ poor end of the MORB regression line, all the others lie on the arc regression line or in the transition zone (Fig. 11A). Similarly, the calculated melts of the chromitites display an arc affinity in the TiO$_{2(melt)}$ vs. TiO$_{2(spinel)}$ diagram, although the two fields largely overlap in their transition zone (Fig. 11B).
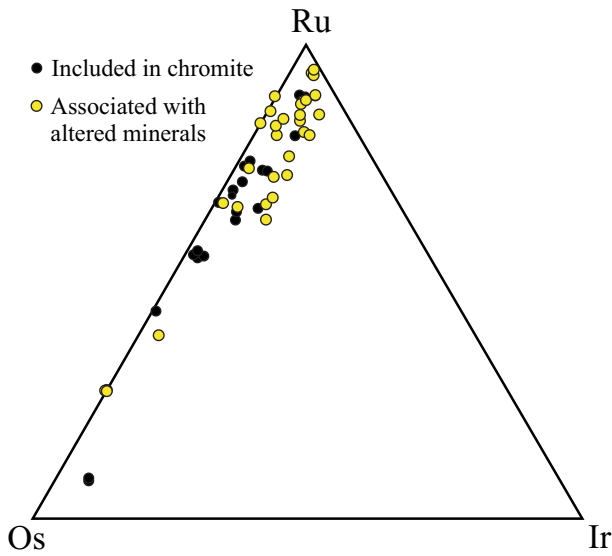
FIGURE 9 | **Electron microprobe composition (Atomic %) of Platinum-group mineral sulfides of the laurite-erlichmanite series, associated with the chromitites of Santa Elena. Both suites of PGM included in chromite or associated with altered minerals show consistent composition.**

Rollinson (2008) has shown that Al-rich and Cr-rich chromitites within the same mantle section of the Oman ophiolite complex may have derived from successive intrusions of MORB and boninitic magmas, characterized by distinct intervals of change in Al_2O_3 concentrations. In contrast, the parental melts of Santa Elena chromitites define a continuous trend from Al_2O_3-poor to relatively Al_2O_3-rich compositions (Figs. 11A and B), and suggest differentiation of a single melt with an initial composition well within the arc field.

Control on Platinum Group Elements distribution and Platinum Group Minerals mineralogy in Santa Elena chromitites

There is a general consensus that high-Cr (Cr/(Cr+Al)>0.70) podiform chromitites that crystallized from boninitic melts in supra subduction zone settings have PGE patterns characterized by high (Os+Ir+Ru)/(Rh+Pt+Pd) ratios and have very low Pd+Pt content (Economou-Eliopoulos, 1996; Zhou et al., 1998; Proenza et al., 1998, 1999; Melcher et al., 1999). Conversely, high-Al (Cr/(Cr+Al)<0.60) chromitite precipitated from MORB may be extremely depleted in PGE with respect to the Cr-rich, having overall flat, or slightly negative chondritic patterns. These variations are strictly related to sulfur saturation in the melt during chromite precipitation (Naldrett and Von Gruenewaldt, 1989; Leblanc, 1991; Garuti, 2004). Boninites are probably the most sulfur undersaturated mafic magmas, because they have formed from a severely depleted mantle source that has lost most, if not all of its original sulfide

phase (Zhou et al., 1998). This implies that the condition of sulfur saturation rarely occurs during crystallization of Cr-rich chromitite within an ophiolitic mantle. In the case of low degrees of melting, the chalcophile Rh, Pt, and Pd (PPGE) are forced to remain in the melt, whereas the high-refractory and siderophile Os, Ir, and Ru (IPGE) are removed from the melt and trapped as nano-sized crystals in precipitating chromite. MORB-like tholeiitic magmas are generated by low degrees of partial melting of primitive mantle. They are believed to be sulfur saturated at the time of their formation, thereby leaving a PGE-bearing sulfide phase in the residual mantle. These melts will generate Al-rich chromitites; generally PGE depleted with slightly negative chondritic patterns (Zhou et al., 1998).

The chondrite-normalized PGE patterns of the Santa Elena chromitites are similar to those of high-Cr chromitites precipitating from boninitic melts (Zhou et al., 1998), regardless of their Cr-rich or Al-rich composition. This similarity supports the view that all the chromitites were derived from a common parental melt with a boninitic PGE signature, but also indicates that there was no apparent fractionation between IPGE and PPGE during melt differentiation and fractional precipitation of the chromitites. We suggest that this was possible if the PGE content of the invading melt precipitating chromite was continuously buffered by reaction with a depleted mantle representing an infinite reservoir of PGE, although at low concentrations, compared with the small volume of infiltrating melt. The observation that the PGE patterns of
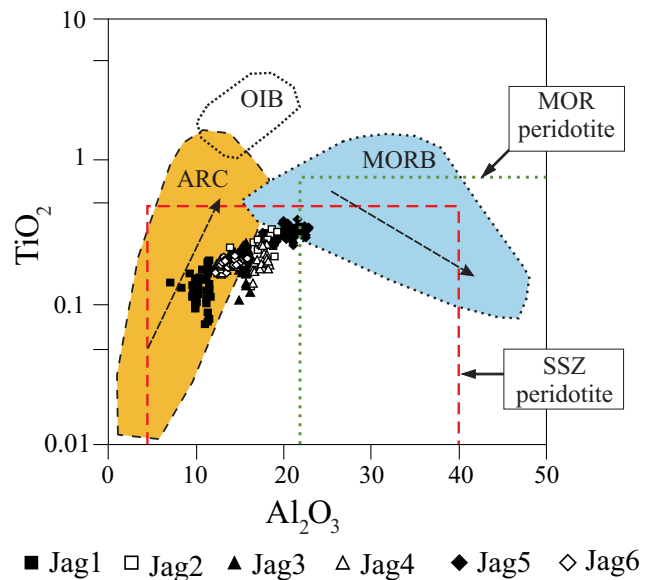

FIGURE 10 | **Al_2O_3-TiO_2 relationships in the chromitites of Santa Elena, compared with compositional fields of spinels from different types of basalts (MORB, OIB, Island Arc) and mantle peridotite in SSZ (supra subduction zone) and MOR settings. Note the contrasting trend in MORB and Island Arc basalts.**

chromitite and mantle peridotite have similar Ru and Pt anomalies strongly supports the hypothesis of melt/country rock interaction.

Mineralogy and textural relations indicate that most of the PGM in the Santa Elena chromitite have crystallized at high magmatic temperatures, prior to or concomitant with precipitation of chromite. Experimental data (Brenan and Andrews, 2001) supported by a large number of natural observations (Augé and Johan, 1988; Melcher et al., 1997; Garuti et al., 1999a, b; Uysal et al., 2007; El Ghorfi et al., 2008; Kapsiotis et al., 2009) indicate that laurite

is in equilibrium with Os-Ir-(Ru) alloys at a temperature of 1300°C and relatively low sulfur fugacity. Laurite becomes progressively enriched in Os with decreasing temperature and increasing sulfur fugacity, up to the stability field of erlichmanite. At Santa Elena, the primary mineral assemblage is dominated by sulfides of the laurite-erlichmanite series, suggesting that sulfur fugacity, although well below the sulfur saturation threshold, was as high as to prevent precipitation of Os-Ir-(Ru) alloys at high temperature.

This feature may not be readily reconciled with the inferred low sulfur fugacity condition of boninites. If this is the case, then addition of sulfur from an external source has to be admitted to explain the PGM assemblage dominated by sulfides observed in the chromitites of Santa Elena. We suggest that the boninitic melt might have assimilated some relic sulfide phase during interaction within the country rock mantle peridotite.

CONCLUDING REMARKS

1) Morphology and size of the ore bodies coupled with field relations (i.e. contact with peridotite) indicate that the chromitites of Santa Elena are magmatic accumulations of chromite along conduits, extending over a short stratigraphic interval in depleted harzburgitic mantle. Lago et al. (1982) described a mechanism of podiform chromitite in which mafic magmas, derived from a deep mantle source, migrate upward through narrow conduits (<50cm) precipitating chromite in relatively large magma chambers (up to 200m high and 5m thick) within the upper mantle tectonite (Fig. 12A). The thermal gradient between up-streaming melts and country rocks, generates turbulent convective cells, in which pristine chromite nuclei are kept in suspension and can agglomerate to form large chromite aggregates. Coarse chromite aggregates sink to the bottom of the chamber, causing progressive plugging of the conduit with the formation of a massive podiform chromitite body.

2) Santa Elena represents a rare example of podiform chromitites in which chromite composition varies from Cr-rich/Ti-poor to relatively rich in Al and Ti, over a short distance within the same mantle block. This feature suggests that the different chromitites might have derived from the fractional crystallization of a single batch of magma. The injected magma had an initial boninitic composition and yielded high-Cr chromite similar to sample Jag-1 (Fig. 12A). Progressive fractionation of Cr-rich chromite produced a weak Al and Ti enrichment in the residual melt that migrated upward and, by mixing with fresh injected magma, precipitated chromite with a slightly higher Al/Cr ratio and Ti content in a next chamber (Fig. 12A).
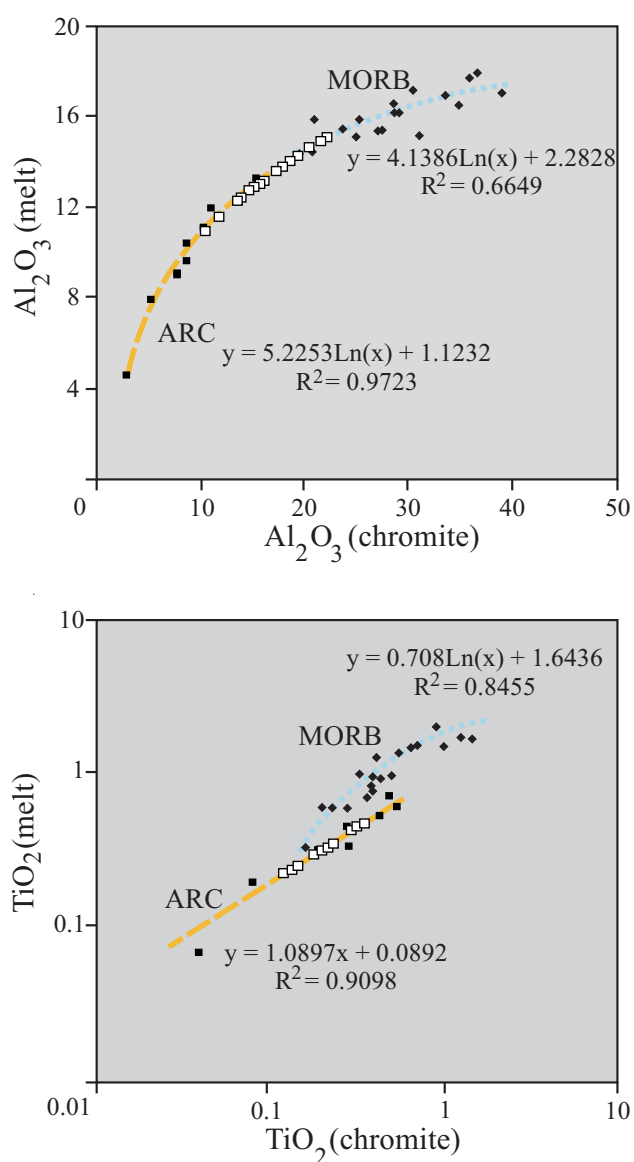

FIGURE 11 | **Graphic plots of calculated Al$_2$O$_3$-TiO$_2$ composition of melts in equilibrium with Santa Elena chromitite (open square, data from Table 2), compared with spinel-melt relationship for MORB (filled square) and ARC (filled diamond) lavas from Table 3, in Kamenetsky et al. (2001). Calculated equations for best fit regression lines are shown.**

|419|

3) Important chemical variations in the boninitic melt can also be induced by reaction with the mantle country rock. At Santa Elena, the geochemical behaviour of PGE and the mineralogy of primary PGM inclusions in chromite are strong evidence supporting the influence of a melt/rock interaction process. The initial boninitic melt was sulfur depleted and probably carried significant PGE, as suspended metallic clusters (Tredoux et al., 1995). The lack of fractionation between IPGE and PPGE and the

sulphide nature of the PGM indicate that small amounts of sulfur and PGE were continuously supplied to the melt by metasomatic reaction with the depleted mantle (Fig. 12A). The presence of analogous Ru and Pt-Pd anomalies in both the chromitite and the mantle peridotite supports this conclusion.

4) Santa Elena chromitites (and their calculated parent melts) have island arc signatures in terms of their TiO_2 vs. Al_2O_3 relation, and correspond to spinels from a supra subduction zone depleted mantle harzburgite, rather than to a MOR type mantle peridotite. These compositional characteristics support the proposition of Gazel et al. (2006) and Denyer and Gazel (2009) that the petrologic evolution of this portion of oceanic lithosphere largely occurred in a supra subduction zone setting (Fig. 12B), apparently independent from intra-oceanic spreading centers or mantle plumes as previously suggested (Beccaluva et al., 1999; Giunta et al., 2006).
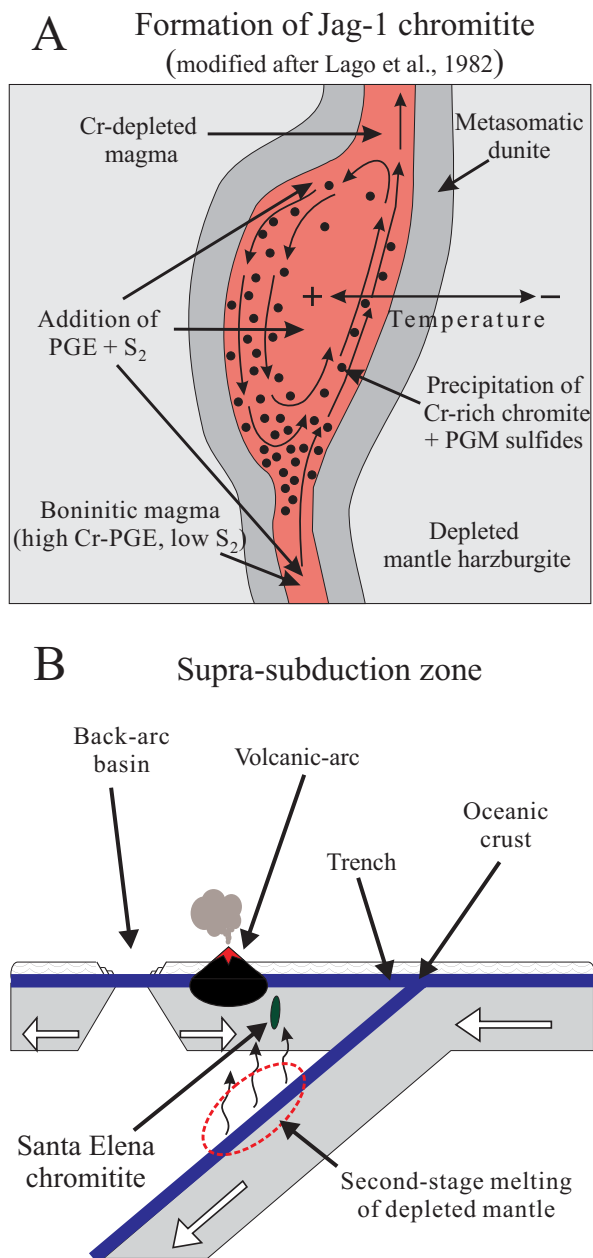
ACKNOWLEDGMENTS

REFERENCES

Álvarez, J., 1987. Mineralogía y química de los depósitos de cromita podiforme de las dunitas de Medellín, Departamento de Antioquía, Colombia. Boletín Geológico, 33(1-3), 34-46.

Augé, T., Johan, Z., 1988. Comparative study of chromite deposits from Troodos, Vourinos, North Oman and New Caledonia ophiolites. In: Boissonas, J., Omenetto, P. (eds.). Mineral deposits within the European Comunity. Society for Geology Applied to Mineral Deposits, 6 (Special Publications), 267-288.

Barnes, S.J., Roeder, L.P., 2001. The Range of Spinel Compositions in Terrestrial Mafic and Ultramafic Rocks. Journal of Petrology, 42, 2279-2302.

Baumgartner, P.O., Denyer, P., 2006. Evidence for Middle Cretaceuos accretion at Santa Elena Peninsula (Santa Rosa Accretionary complex), Costa Rica. Geologica Acta, 4(1-2), 179-191.

Baumgartner, P.O., Flores, K., Bandini, A.N., Girault, F., Cruz, D.,

FIGURE 12 | **Synoptic cartoon illustrating A) the mechanism of formation and B) the general geodynamic setting proposed for the origin of small chromitite bodies within the depleted harzburgite mantle of Santa Elena.**

2008. Upper Triassic to Cretaceous radiolara from Nicaragua and northern Costa Rica - The Mesquito composite oceanic terrane. Ofioliti, 33, 1-19.

Beccaluva, L., Chinchilla-Chaves, A.L., Coltorti, M., Giunta, G., Siena, F., Vaccaro, C., 1999. Petrological and structural significance of the Santa Elena-Nicoya ophiolitic complex in Costa Rica and geodynamic implications. European Journal of Mineralogy, 11, 1091-1107.

Beeson, M.H., Jackson, E.J., 1969. Chemical composition of altered chromites from the Stillwater Complex, Montana. American Mineralogist, 54, 1084-1100.

Brenan, J.M., Andrews, D.R.A., 2001. High-temperature stability of laurite and Ru-Os-Ir alloys and their role in PGE fractionation in mafic magmas. The Canadian Mineralogist, 39, 341-360.

Buenaventura, J., 2001. Memoria explicativa del mapa de recursos minerales de Colombia: minerales metálicos, preciosos y energéticos a escalas 1:500.000. Subdirección de recursos del subsuelo. República de Colombia, Ministerio de Minas y Energía, Instituto de Investigación e Información Geocientífica, Minero Ambiental y Nuclear, Ingeominas, 64pp.

Denyer, P., Baumgartner, P.O., Gazel, E., 2006. Characterization and tectonic implications of Mesozoic-Cenozoic oceanic assemblage of Costa Rica and Western Panama. Geologica Acta, 4(1-2), 219-235.

Denyer, P., Gazel, E., 2009. The Costa Rican Jurassic to Miocene oceanic complexes: origin, tectonics and relations. Journal of South American Earth Sciences, 28, 429-442.

Dick, H.J.B., Bullen, T., 1984. Chromian spinel as a petrogentic indicator in abyssal and alpine-type peridotites and spatially associated lavas. Contributions to Mineralogy and Petrology, 86, 54-76.

Dickey, J.S.Jr., 1975. A hypothesis of origin for podiform chromite deposits. Geochimica et Cosmochimica Acta, 39, 1061-1074.

Economou-Eliopoulos, M., 1996. Platinum group element distribution in chromite ores from ophiolite complexes: implication for their exploration. Ore Geology Reviews, 11, 363-381.

El Ghorfi, M., Melcher, F., Oberthur, T., Boukhari, A.E., Maacha, L., Maddi, A., Mhaili, M., 2008. Platinum group minerals in podiform chromitites of Bou Azzer ophiolite, Anti Atlas, Central Morocco. Mineralogy and Petrology, 92, 59-80.

Flores, K., Baumgartner, P.O., Skora, S., Baumgartner, L., Muntener, O., Cosca, M., Cruz, D., 2007. The Siuna Serpentinite Melange: An Early Cretaceous Subduction/Accretion of a Jurassic Arc. San Francisco (USA), American Geophysical Union, Fall Meeting 10-14 December 2007, abstract, T11D-03.

Friedrich, G., Brunemann, H.G., Wilcke, J., Stumpfl, E.F., 1980. Chrome spinels in lateritic soils and ultramafic source rocks, Acoje Mine, Zambales, Philippines. In: Jankovic, S., Petrasheck, W.E. (eds.). An International symposium on metallogeny of mafic and ultramafic complexes: the eastern Mediterranean-western Asian area, and its comparison with similar metallogenic environments in the world. Athens, 9-11 October 1980, UNESCO-IGCP n° 1691, 257-278.

Garuti, G. 2004. Chromite-Platinum Group Element magmatic deposits. In: De Vivo, B., Stüwe, K. (eds.). Geology, Encyclopedia of Life Support Systems (EOLSS). Oxford (United Kingdom), UNESCO, Eolss Publisher, http://www.eolss.net.

Garuti, G., Economou-Eliopoulos, M., Zaccarini, F., 1999a. Paragenesis and composition of laurite from the chromitites of Othrys (Greece): implications for Os-Ru fractionation in upper mantle of the Balkan peninsula. Mineralium Deposita, 34, 312-319.

Garuti, G., Pushkarev, E.V., Zaccarini, F., 2005. Diversity of chromite-PGE mineralization in ultramafic complexes of the Urals. In: Törmänen, T.O., Alapieti, T.T. (eds.). Platinum Group Elements – from Genesis to Benefication and Environmental Impact. Oulu (Finland), August 8-11, 10th International Platinum Symposium, extended abstracts, 341-344.

Garuti, G., Zaccarini, F., Moloshag, V., Alimov, V., 1999b. Platinum group minerals as indicator of sulfur fugacity in ophiolitic upper mantle: an example from chromitites of the Ray-Iz ultramafic complex, Polar Urals, Russia. The Canadian Mineralogist, 37, 1099-1115.

Gazel, E., Denyer, P., Baumgartner, P.O., 2006. Magmatic and geotectonic significance of Santa Elena Peninsula, Costa Rica. Geologica Acta, 4(1-2), 193-202.

Giunta, G., Beccaluva L., Siena, F., 2006. Caribbean Plate margin evolution: constraints and current problems. Geologica Acta, 4(1-2), 265-277.

Hauff, F., Hoernle, K., Bogard, van den P., 2000. Age and geochemistry of basaltic complexes in western Costa Rica: Contribution to the geotectonic evolution of Central America. Geochemistry Geophysics Geosystems, 1, doi: 1999GC000020.

Jager-Contreras, G., 1977. Geología de las mineralizaciones de cromita al Este de la Península de Santa Elena, Provincia de Guanacaste, Costa Rica. In Spanish. Doctoral Thesis. San José (Costa Rica), University of Costa Rica, 136pp.

Kapsiotis, A., Grammatikopoulos, T., Tsikouras, V., Hatzipanagiotou, Zaccarini, F., Garuti, G., 2009. Chromian spinel composition and Platinum group element mineralogy of chromitites from the area of Milia, Pindos ophiolite complex, Greece. The Canadian Mineralogist, 47, 883-902.

Kamenetsky, V.S., Crawford, A.J., Meffre, S., 2001. Factors controlling chemistry of magmatic spinel: an empirical study of associated olivine, Cr-spinel and melt inclusions from primitive rocks. Journal of Petrology 42, 655-671.

Kocks, H., Melcher, F., Meisel, T., Burgath, K.-P., 2007. Diverse contributing sources to chromite petrogenesis in the Shebenik Ophiolitic Complex, Albania: evidence from new PGE- and Os-isotope data. Mineralogy and Petrology, 91, 139-170.

Kuipjers, E.P., Jager-Contreras, G., 1979. Mineralizaciones de cromita en la Península de Santa Elena, Costa Rica. In Spanish. Ciencia Técnica, 3, 99-108.

Irvine, T.N., 1965. Chromian spinel as a petrogenetic indicator. Part I. Theory. Canadian Journal of Earth Sciences, 2, 648-672.

Irvine, T.N., 1967. Chromian spinel as a petrogenetic indicator. Part II. Petrological Application. Canadian Journal of Earth Sciences, 4, 71-103.

Lago, B.L., Rabinowicz, M., Nicolas, A., 1982. Podiform chromite ore bodies: a genetic model. Journal of Petrology, 23, 103-125.

Leblanc, M., 1991. Platinum group and gold in ophiolitic complexes: Distribution and fractionation from mantle to oceanic floor. In: Peters, Tj., Nicolas, A., Coleman, R. (eds.). Ophiolite genesis and evolution of the oceanic lithosphere. Ministry of Petroleum and Minerals, Sultanate of Oman, 231-260.

Leblanc, M., 1995. Chromitite and ultramafic rock compositional zoning through a Paleotransform fault, Poum, New Caledonia. Economic Geology, 90, 2028-2039.

Leblanc, M., Nicolas, A., 1992. Ophiolitic chromitites. International Geology Review, 34(7), 653-686.

Maurel, C., Maurel, P., 1982. Étude experimental de la distribution de l'aluminium entre bain silicate basique et spinel chromifere. Implications pétrogenetiques: tenore en chrome des spinelles. Bulletin de Mineralogie, 105, 197-202.

Melcher, F., Grum, W., Simon, G., Thalhammer, T.V., Stumpfl, F.E., 1997. Petrogenesis of the ophiolitic giant chromite deposits of Kempirsai, Kazakhstan: a study of solid and fluid inclusions in chromite. Journal of Petrology, 38, 1419-1438.

Melcher, F., Grum, W., Thalhammer, T.V., Thalhammer, O.A.R., 1999. The giant chromite deposits at Kempirsai, Urals: constraints from trace element (PGE, REE) and isotope data. Mineralium Deposita, 34, 250-272.

Naldrett, A.J., Duke, J.M., 1980. Pt metals in magmatic sulfide ores. Science, 208, 1417-1424.

Naldrett, A.J., von Gruenevaldt, G., 1989. Association of platinum group elements with chromitite in layered intrusions and ophiolite complexes. Economic Geology, 84, 180-187.

Proenza, J.A., Zaccarini, F., Lewis, J.F., Longo, F., Garuti, G., 2007. Chromian spinel composition and the Platinum Group Minerals of the PGE-rich Loma Peguera chromitites, Loma Caribe peridotite, Dominican Republic. The Canadian Mineralogist, 45, 211-228.

Proenza, J.A., Melgarejo, J.C., 1998. Una introdución a la metalogenia de Cuba bajo la perspectiva de la tectónica de placas. Acta Geologica Hispanica, 33, 89-132

Proenza, J.A., Gervilla, F., Melgarejo, J.C., Reve, D., Rodríguez, Y.G., 1998. Ophiolitic chromitites from the Mercedita deposit (Cuba). Example of Al-rich chromites at the mantle-crust transition zone. Acta Geologica Hispanica, 33, 179-212.

Proenza, J.A., Gervilla, F., Melgarejo, J.C., Bodinier, J.L., 1999. Al and Cr rich chromitites from the mayari-Baracoa Ophiolitic Belt, (eastern Cuba): consequence of interaction between volatile-rich melts and peridotite in suprasubduction mantle. Economic Geology, 94, 547-566.

Proenza, J.A., Escayola, M., Ortiz, F., Pereira, E., Correa, A.M., 2004. Dunite and associated chromitites from Medellín (Colombia). Florence (Italy), 32nd International Geological Congress, Abstract volume, CD-ROM.

Rodríguez, S., 1986. Recursos Minerales de Venezuela. Caracas, Boletín del Ministerio de Energía y Minas, 15(27), 215pp.

Roeder, P.L., 1994. Chromite: from the fiery rain of chondrules to the Kilauea Iki lava lake. The Canadian Mineralogist, 32, 729-746.

Rollinson, H., 2008. The geochemistry of mantle chromitites from the northern part of the Oman ophiolite: inferred parental melt composition. Contributions to Mineralogy and Petrology, 156, 273-288.

Savelieva, G.N., 2004. Chromite of the Polar Urals. In Pecchio, M., Andrade, F.R.D., D'Agostino, L.Z., Kahn, H., Sant'Agostino, L.M., TassinarI, M.M.M.L. (eds.). Applied Mineralogy: Developments in Science and Technology. Águas de Lindoia (Brazil), 19-24 September 2004, Proceedings International Congress on Applied Mineralogy ICAM 2004, 943-945.

Stowe, C.W., 1994. Compositions and tectonic settings of chromite deposits through time. Economic Geology, 89, 528-546.

Thayer, T.P., 1946. Preliminary chemical correlation of chromite with the containing rocks. Economic Geology, 41, 202-217.

Thayer, T.P., 1970. Chromite segregations as petrogenetic indicators. The Geological Society of South Africa, 1 (Special Publications), 380-390.

Tournon, J., 1994. The Santa Elena Peninsula: an ophiolitic nappe and a sedimentary volcanic relative autochthonous. Profil, 7, 87-96.

Tredoux, M., Lindsay, N.M., Davies, G., McDonald, I., 1995. The fractionation of platinum group elements in magmatic system, with the suggestion of a novel causal mechanism. South African Journal of Geology, 98, 157-167.

Uysal, I., Zaccarini, F., Garuti, G., Meisel, T., Tarkian, M., Bernhardt, H.J., Sadiklar, M.B., 2007. Ophiolitic chromitites from the Kahramanmaras area, southeastern Turkey: their platinum group elements (PGE) geochemistry, mineralogy and Os-isotope signature. Ofioliti, 32, 151-161.

Uysal, I., Zaccarini, F., Sadiklar, M.B., Tarkian, M., Thalhammer, O.A.R., Garuti, G., 2009a. The podiform chromitites in the Dağküplü and Kavak mines Eskişeir ophiolite (NW-Turkey): Genetic implications of mineralogical and geochemical data. Geologica Acta, 7(3), 351-362.

Uysal, I., Tarkian, M., Sadiklar, M.B., Zaccarini, F., Meisel, T., Garuti, G., Heidrich, S. 2009b. Petrology of Al- and Cr-rich ophiolitic chromitites from the Muğla, SW Turkey: implications from composition of chromite, solid inclusions of platinum group mineral, silicate, and base-metal mineral, and Os-isotope geochemistry. Contributions to Mineralogy and Petrology, 158, 659-674.

Zaccarini, F., 2005. Compositions of chromitite and associated solid inclusions: a key to understanding mantle and derived magmas. In Italian. Doctoral Thesis. Italy, University of Modena and Reggio Emilia, unpublished, 76pp.

Zaccarini, F., Proenza, A.J., Ortega-Gutierrez, F., Garuti, G., 2005. Platinum group minerals in ophiolitic chromitites from Tehuitzingo (Acatlan complex, southern Mexico): implications for post-magmatic modification. Mineralogy and Petrology, 84, 147-168.

Zaccarini, F., Proenza, J.A., Rudashevsky, N.S., Cabri, L.J., Garuti, G., Rudashevsky, V.N., Melgarejo, J.C., Lewis, J.F., Longo, F., Bakker, R., Stanley, C.J., (2009). The Loma Peguera ophiolitic chromitite (Central Dominican republic): a source of new platinum group minerals (PGM) species. Neues Jahrbuch für Mineralogie Abhandlungen, 185(3), 335-349.

Zhou, M.-F., Bai, W.-J., 1992. Chromite deposits in China and their origin. Mineralium Deposita, 27, 192-199.

Zhou, M.-F., Robinson, P.T., 1997. Origin and tectonic environment of podiform chromite deposits. Economic Geology, 92, 259-262.

Zhou, M.-F., Sun, M., Keays, R.R., Kerrich, R.W., 1998. Controls on platinum group elemental distributions of podiform chromitites: A case study of high-Cr and high-Al chromitites from Chinese orogenic belts. Geochimica et Cosmochimica Acta, 62(4), 677-688.